BIBECHANA
Vol. 21, No. 3, December 2024,300-310

ISSN 2091-0762 (Print), 2382-5340 (Online)
Journal homepage: http://nepjol.info/index.php/BIBECHANA
Publisher: Dept. of Phys., Mahendra Morang A. M. Campus (Tribhuvan University) Biratnagar

Effect of blood flow through mild stenosed artery with effective viscosity

Bishnu Prasad Bhandari[1,2], Jeevan Kafle[1], Chudamani Pokharel[1,3,*]

[1] *Central Department of Mathematics, Tribhuvan University, Kathmandu, Nepal*
[2] *Nepal Engineering College, Pokhara University, Changunarayan, Bhaktapur, Nepal*
[3] *Dhawalagiri Multiple Campus, Tribhuvan University, Kathmandu, Nepal*

[*]Corresponding author: Email: chuda.pokherel@dmc.tu.edu.np

Abstract

Normal blood flow is disrupted by aortic stenosis, which raises risks and affects the cardiovascular system. This work analyzes blood viscosity from the central core line to the arterial wall in order to look at flow parameters in arteries with minor stenosis. In order to account for effective viscosity at radial distances, fluid dynamics in axisymmetric directions are analyzed using the Navier-Stokes equation. Additionally, analytical expressions for shear stress, pressure drop, velocity profile, and volumetric flow rate are investigated. These results contribute to our growing knowledge of vascular physiology in stenosis and emphasize the intricacy of blood flow dynamics.

Keywords
Arterial Stenosis, Viscosity, Hematocrit, Hemodynamic parameters.

Article information
Manuscript received: April 2, 2024; Revised: June 23, 2024; Accepted: June 24, 2024
DOI https://doi.org/10.3126/bibechana.v21i3.64409

1 Introduction

Atherosclerotic plaque is formed by the accumulation of cholesterol, fat, and other foreign particles [1]. Arteriosclerosis, specifically the abnormal thickening and hardening of the artery walls, significantly impacts the cardiovascular system. This condition can result from various poor lifestyle choices, such as smoking, physical inactivity, and an unhealthy diet. The progression of arteriosclerosis leads to notable changes in hemodynamic parameters, including flow resistance, wall shear stress, pressure distribution, and blood flow [2, 3]. Stenosis in an artery often results from the accumulation of cholesterol-rich particles, leading to the formation of atherosclerotic plaques. These plaques build up on the interior walls of arteries, causing several detrimental effects [4]. Heart diseases and stroke are significant global health issues, contribut-

ing to high mortality rates [5]. When analyzing medical imaging results like angiograms or ultrasound scans, different types of stenosis shapes can indeed have specific hemodynamic implications, affecting the severity and consequences of blood flow obstruction [6]. Theoretical and experimental investigations into the effects of restrictions on blood flow parameters are crucial for understanding the hemodynamics of blood flow in both physiological and pathological conditions [7–9].

Hematocrit is a significant factor that influences blood viscosity. Additional features that can raise blood viscosity include decreased red blood cell deformability, high red blood cell aggregation, and increased plasma viscosity [10–12]. Blood velocity and hematocrit percentage are two significant factors that have been shown to influence wall shear stress in the blood flow through a tapered artery [13]. A complete blood count (CBC) is a comprehensive examination that identifies and tracks various medical disorders by analyzing hematocrit concentration, white blood cell count, and platelet count [2,14]. Examined the effects of pressure gradients, wall shear stress, blood velocity, and volumetric flow rate on human carotid arteries. An increase in the hematocrit and viscosity is accompanied by a decrease in the artery wall shear stress, indicating an increase in heart rate [15]. These results highlight the way that hematocrit, catheter size, and stenosis interact to influence blood flow hemodynamics. It has been found that the impedance changes with the size of the stenosis, hematocrit, and catheter [12]. Blood clotting in the human heart can be fatal, as evidenced by the correlation between hematocrit and blood pressure gradient [14]. If platelets are activated by exceptionally high shear stress near the top of the stenosis, such atherosclerosis damages the cardiovascular system by entirely blocking blood flow to the heart [16].

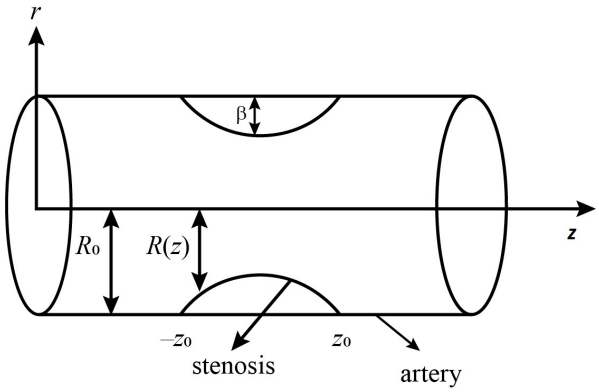

Figure 1: Schematic illustration of a stenotic artery.

Mandal and Chakravarty [17] have shown that blood behaves like a non-Newtonian fluid in arteries with small radii and at low shear rates. According to Chaturani and Ponalagusamy [18] blood exhibits complex rheological behavior, particularly at low shear rates, where it demonstrates a non-zero yield stress. This phenomenon is primarily due to the interactions between erythrocytes (red blood cells), which can aggregate to form structures known as rouleaux. Singh et al. [16] assumed a little asymmetric stenosis along the radial direction. Biswas and Chakraborty [13] examined the pulsatile blood flow across a moderately stenotic tapering artery with slip velocity at the arterial wall. Haldar et al. [19] have investigated the effects of blood viscosity, wall shear stress, velocity, and hematocrit percentage on blood flow in the stenosed artery. Bali and Awasthi [20] determined how blood viscosity varies with hematocrit and distance from the center, and how the external magnetic field affects the flow. Onitilo and Usman [14] examined the theory that arterial wall shear stress would be decreased by raising hematocrit and viscosity.

The literature review that was previously discussed offers proof of the impact that stenosis has on blood flow. In this study, blood flow characteristics with mild stenosis were examined in relation to blood viscosity in plasma, hematocrit, and the site of stenosis. The cylindrical polar form of the Navier-Stokes equation has been applied in axisymmetric directions.

2 Methods

Considering the constant blood flow in an axially symmetrical artery that has stenosis. Let R_0 and R represent the artery's radius in the absence and presence of stenosis, respectively. The artery is viewed as a circular, inelastic tube. With stenosis, the radial blood flow is disregarded. Blood is thought to flow exclusively in an axial direction.

2.1 Model Equation

Considering the three components of velocity and pressure at (x, y, z) and at time t are $u(x, y, z, t)$, $v(x, y, z, t)$, $w(x, y, z, t)$ and $p(x, y, z, t)$ respectively. The continuity equation in a steady-state form is [4, 21]

$$\frac{\partial u}{\partial x} + \frac{\partial v}{\partial y} + \frac{\partial w}{\partial z} = 0. \tag{1}$$

Here, a fluid's density is represented by $\rho(x, y, z, t)$. An incompressible viscous fluid has a constant density, ρ. The Newtonian, viscous, and incompressible fluid N-S equations are [4, 21]

$$\rho\left(\frac{\partial u}{\partial t}+u\frac{\partial u}{\partial x}+v\frac{\partial u}{\partial y}+w\frac{\partial u}{\partial z}\right)=\rho g_x-\frac{\partial p}{\partial x}+\mu\left(\frac{\partial^2 u}{\partial x^2}+\frac{\partial^2 u}{\partial y^2}+\frac{\partial^2 u}{\partial z^2}\right) \tag{2}$$

$$\rho\left(\frac{\partial v}{\partial t}+u\frac{\partial v}{\partial x}+v\frac{\partial v}{\partial y}+w\frac{\partial v}{\partial z}\right)=\rho g_y-\frac{\partial p}{\partial y}+\mu\left(\frac{\partial^2 v}{\partial x^2}+\frac{\partial^2 v}{\partial y^2}+\frac{\partial^2 v}{\partial z^2}\right) \tag{3}$$

$$\rho\left(\frac{\partial w}{\partial t}+u\frac{\partial w}{\partial x}+v\frac{\partial w}{\partial y}+w\frac{\partial w}{\partial z}\right)=\rho g_z-\frac{\partial p}{\partial z}+\mu\left(\frac{\partial^2 w}{\partial x^2}+\frac{\partial^2 w}{\partial y^2}+\frac{\partial^2 w}{\partial z^2}\right). \tag{4}$$

In this case, t represents the time, and the external body forces, namely gravity, are $f=\rho(g_x,\, g_y,\, g_z)$. The forces resulting from pressure differences are denoted by the terms $\partial p/\partial x$, $\partial p/\partial y$, $\partial p/\partial z$, and the viscous forces with constant viscosity coefficient μ in the x, y, and z- direction are represented by the last term on the right. The system (1)-(4) is closed for four unknown functions u, v, w and p. If $g_x=0$, $g_y=0$, and $g_z=0$ are the only external body forces acting on the motion, and if the motion is steady—that is, not changing over time—then $\partial u/\partial t=0$, $\partial v/\partial t=0$, $\partial w/\partial t=0$, and $\partial p/\partial t=0$, and the motion is two-dimensional.

The Navier-Stokes equations for fluid flow inside a cylinder can be used to predict the flow of blood through arteries. We will use r and p to represent the artery's blood flow's radius and pressure drop. The velocities' components along the radial, angular, and axial directions are v^r, v^θ, and v^z, individually. The system (1)-(4) can be expressed in cylindrical form using $x=r\cos\theta$, $y=r\sin\theta$, $r^2=x^2+y^2$ and $\theta=\tan^{-1}(y/x)$ from Cartesian coordinate (x,y,z) to polar coordinate (r,θ,z). The equation of continuity and the equation of motion are [3, 21]

$$\frac{1}{r}\frac{\partial}{\partial r}(rv^r)+\frac{\partial}{\partial z}(v^z) = 0 \tag{5}$$

$$\rho\left(\frac{\partial v^r}{\partial t}+v^r\frac{\partial v^r}{\partial r}+v^z\frac{\partial v^r}{\partial z}\right) = -\frac{\partial p}{\partial r}+\mu\left(\frac{\partial^2 v^r}{\partial r^2}+\frac{\partial^2 v^r}{\partial z^2}+\frac{1}{r}\frac{\partial v^r}{\partial r}-\frac{v^r}{r^2}\right) \tag{6}$$

$$\rho\left(\frac{\partial v^z}{\partial t}+v^r\frac{\partial v^z}{\partial r}+v^z\frac{\partial v^z}{\partial z}\right) = -\frac{\partial p}{\partial z}+\mu\left(\frac{\partial^2 v^z}{\partial r^2}+\frac{\partial^2 v^z}{\partial z^2}+\frac{1}{r}\frac{\partial v^z}{\partial r}\right) \tag{7}$$

We assume $v^\theta=0$ in the axisymmetric flow, and p, v^r, and v^z are independent of θ. For a steady flow of blood, viscosity μ and density ρ are considered to be constant. v is the velocity component parallel to the z-axis. Only axially symmetric flow along the z-axis has been examined, therefore if $v^r=0$, $v^\theta=0$, and $v^z=v$, then equations (6) - (7) become

$$\frac{\partial v}{\partial z} = 0, \quad 0=-\frac{\partial p}{\partial r}, \quad 0=-\frac{\partial p}{\partial z}+\mu\left(\frac{\partial^2 v}{\partial r^2}+\frac{\partial^2 v}{\partial z^2}+\frac{1}{r}\frac{\partial v}{\partial r}\right) \tag{8}$$

Suppose pressure term as $P(z)=-\partial p/\partial z$, equation (8) reduces to

$$-P(z)\frac{r}{\mu}=\frac{\partial}{\partial r}\left(r\frac{\partial v}{\partial r}\right). \tag{9}$$

At a radial distance r, the effective viscosity of blood is expressed as [2, 22].

$$\mu_r=\mu_p\left[1+\alpha H_r\right] \tag{10}$$

where μ_p is a plasma viscosity, α is a constant that characterizes the dependence of viscosity on hematocrit, H_r is the hematocrit at radial distance r, and αH_r reflects the increased viscosity due to the presence of red blood cells. The formula describes this relationship.

$$H_r=\mathcal{H}\left[1-\left(\frac{r}{R_0}\right)^m\right] \tag{11}$$

here, m is the number of stenosis, $m=1$ is used

from (10) and (11)

$$\mu_r=\mu_p\left[1+\alpha\mathcal{H}-\alpha\mathcal{H}\left(\frac{r}{R_0}\right)\right]$$

put $b_2 = \alpha\mathcal{H}$, $b_1 = 1 + b_2$

$$\mu_r = \mu_p \left[b_1 - b_2 \left(\frac{r}{R_0} \right) \right] \tag{12}$$

2.2 Geometry of Stenosis

Figure 1 describes the form of the stenosis that results from the layer being deposited inside a cylindrical artery.

$$R = R_0 \left(1 - \frac{\beta}{2R_0} \left(1 + \cos \frac{\pi z}{z_0} \right) \right) \tag{13}$$

where β is the greatest thickness and R and R_0 are the radii with and without stenosis [21].

The boundary condition as stated by [3, 21]

$$v = \begin{cases} 0 & at \ \ r = R, \\ 0 & at \ \ r = R_0, \end{cases}$$

and

$$\frac{\partial v}{\partial r} = 0 \ \text{ at } \ r = 0$$

2.3 Velocity Profile

From equations (9) and (12)

$$\frac{Pr}{\mu_p \left(b_1 - b_2 \left(\frac{r}{R_0} \right) \right)} + \frac{\partial}{\partial r} \left(r \frac{\partial v}{\partial r} \right) = 0$$

$$\frac{Pr}{\mu_p b_1} \left(1 - \frac{b_2 r}{b_1 R_0} \right)^{-1} + \frac{\partial}{\partial r} \left(r \frac{\partial v}{\partial r} \right) = 0.$$

Binomial expansion is used, and neglect the higher power of r,

$$\frac{Pr}{\mu_p b_1} \left(1 + \frac{b_2 r}{b_1 R_0} \right) + \frac{\partial}{\partial r} \left(r \frac{\partial v}{\partial r} \right) = 0.$$

Apply boundary conditions after integration,

$$\frac{\partial v}{\partial r} = -\frac{P}{\mu_p b_1} \left(\frac{r}{2} + \frac{b_2 r^2}{3 b_1 R_0} \right).$$

Again integration,

$$v = -\frac{P}{\mu_p b_1} \left(\frac{r^2}{4} + \frac{b_2 r^3}{9 b_1 R_0} \right) + A(z) \tag{14}$$

used boundary condition, $v = 0$, at $r = R$

$$A(z) = \frac{P}{\mu_p b_1} \left(\frac{R^2}{4} + \frac{b_2 R^3}{9 b_1 R_0} \right)$$

then equation (14) becomes,

$$v = \frac{P}{\mu_p b_1} \left[\frac{1}{4} \left(R^2 - r^2 \right) + \frac{b_2}{9 b_1 R_0} \left(R^3 - r^3 \right) \right]. \tag{15}$$

$$P = \frac{8\mu_p b_1 Q}{\pi R_0^4 \left(1 - \frac{\beta}{2R_0}\left(1 + cos\frac{\pi z}{z_0}\right)\right)^4}\left[1 - \frac{8b_2}{15b_1}\left(1 - \frac{\beta}{2R_0}\left(1 + cos\frac{\pi z}{z_0}\right)\right)\right]$$

Binomial expansion is used, and neglect the higher power of β then it becomes,

$$P = \frac{8\mu_p b_1 Q}{\pi R_0^4}\Big[1 + \frac{2\beta}{R_0}\left(1 + cos\frac{\pi z}{z_0}\right) - \frac{8b_2}{15b_1}\Big(1 + \frac{\beta}{R_0} - \frac{3\beta^2}{2R_0^2} + \left(\frac{\beta}{R_0} - \frac{2\beta^2}{R_0^2}\right)cos\frac{\pi z}{z_0} - \frac{\beta^2}{2R_0^2}cos\frac{2\pi z}{z_0}\Big)\Big]. \tag{19}$$

Pressure drop on the stenosed region is

$$\Delta P = \int_{-z_0}^{z_0} P dz$$

from the equation (19) and then integration, we have

$$\Delta P = \frac{16\mu_p b_1 Q z_0}{\pi R_0^4}\left(1 + \frac{\beta}{R_0} + \frac{3\beta^2}{2R_0^2} - \frac{8b_2}{15b_1}\right) \tag{20}$$

if there is no stenosis i.e., $\beta = 0$ then equation (20) becomes

$$(\Delta P)_p = \frac{16\mu_p b_1 Q z_0}{\pi R_0^4}\left(1 - \frac{8b_2}{15b_1}\right). \tag{21}$$

Ratio of pressure drop is

$$\frac{\Delta P}{(\Delta P)_p} = \frac{\left(1 - \frac{8b_2}{15b_1} + \frac{\beta}{R_0} + \frac{3\beta^2}{2R_0^2}\right)}{\left(1 - \frac{8b_2}{15b_1}\right)} \tag{22}$$

2.6 Ratio of Shear Stress

Kapur and Pokharel et al. [4,21] have mentioned the formula

$$\tau = \frac{PR}{2}.$$

From the equation 14,

$$\tau = \frac{4\mu_p b_1 Q}{\pi R^3}\left(1 - \frac{8b_2 R}{15b_1 R_0}\right)$$

with the help of equation (13), Binomial expansion is used, and neglect the higher power of δ, we get

$$\tau = \frac{4\mu_p b_1 Q}{\pi R_0^3}\left(1 + \frac{3\beta}{2R_0}\left(1 + cos\frac{\pi z}{z_0}\right)\right)\left[1 - \frac{8b_2}{15b_1}\left(1 - \frac{\beta}{2R_0}\left(1 + cos\frac{\pi z}{z_0}\right)\right)\right] \tag{23}$$

if there is no stenosis i.e., $\beta = 0$, then equation (23) becomes,

$$\tau_p = \frac{4\mu_p b_1 Q}{\pi R_0^3}\left(1 - \frac{8b_2}{15b_1}\right) \tag{24}$$

the ratio of shear stress

$$\frac{\tau}{\tau_p} = \frac{\left(1 + \frac{3\beta}{2R_0}\left(1 + cos\frac{\pi z}{z_0}\right)\right)\left[1 - \frac{8b_2}{15b_1}\left(1 - \frac{\beta}{2R_0}\left(1 + cos\frac{\pi z}{z_0}\right)\right)\right]}{\left(1 - \frac{8b_2}{15b_1}\right)} \tag{25}$$

3 Results and Discussion

Computational approaches provide a detailed analysis of blood flow characteristics in stenosed arteries and offer valuable insights into the physiological impacts and potential treatment choices.

3.1 Velocity of blood flow through a stenotic artery

Figure 2(A), explains the relationship between velocity and radius for both effective and plasma viscosity. The effective viscosity is 33.05 mm s^{-1} at the beginning, when $r = 0$, and the plasma viscosity is 47.67 mm s^{-1}. For effective and plasma viscosity receptively, the velocities are 29.82 mm s^{-1} and 43.40 mm s^{-1} for $r = 1$ mm. In a similar vein, an artery's radius is 2 mm, and its effective and plasma viscosity velocities are 19.23 mm s^{-1} and 27.12 mm s^{-1}, respectively. Additionally, it has been noted that velocities stop at an artery's inner wall. According to the above, velocity reaches its maximum in the center and progressively declines towards the wall for every value of plasma viscosity and effective viscosity. This simulation's output demonstrates how effective viscosity has a significant impact on velocity, as seen in the figure. This investigation concludes that the effective viscosity has a greater impact on blood flow velocity than plasma viscosity.

Figure 2(B), shows how the hematocrit affects the velocity profile under the assumption that the pressure drop is constant. We've assumed an artery's radius of 3 mm and pressure of 80 Pa. The velocity drops from 34.96 mm s^{-1} to 19.73 mm s^{-1}, or roughly 15.23 mm s^{-1} at $r = 0$, when the hematocrit rises from 0.2 to 0.8. The velocity falls from 31.34 mm s^{-1} to 17.84 mm s^{-1}, or roughly 13.5 mm s^{-1} at $r = 1$ mm, when the hematocrit rises from 0.2 to 0.8. In a similar manner, the velocity drops from 20.01 mm s^{-1} to 11.51 mm s^{-1}, or roughly 8.42 mm s^{-1} at $r = 2$ mm, when the hematocrit rises from 0.2 to 0.8. Finally, as the picture illustrates, the hematocrit increases somewhat, followed by a quick initial reduction in velocity and a subsequent steady decrease. Near the inner wall of the artery, the velocity is almost zero, and it gradually increases as we move into the center. A low hematocrit causes a quicker rate of velocity rise.

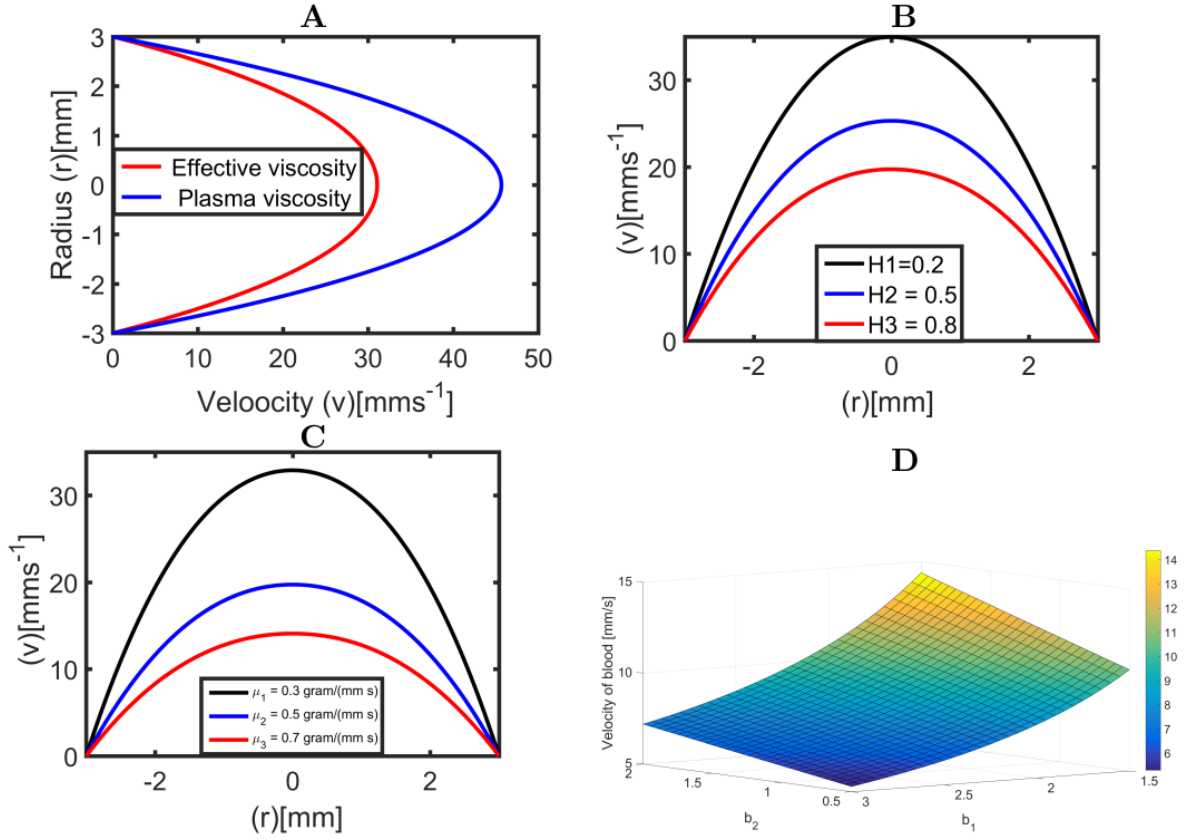

Figure 2: Velocity variations with radial distance for A: comparison viscosity, B: various hematocrit, C: various viscosity, D: increased viscosity due to the presence of red blood cells.

Figure 2(C), shows how viscosity affects the velocity profile under the assumption that the pressure drop is constant. We've assumed that an artery's radius is 3 mm. The velocity drops from 32.89 mm s^{-1} to 14.1 mm s^{-1}, or roughly 24.79 mm s^{-1} at $r = 0$, when the viscosity increases from 0.3 to 0.7. The velocity drops from 29.73 mm s^{-1} to 12.74 mm s^{-1}, or roughly 16.99 mm s^{-1} at $r = 1$ mm, as viscosity increases from 0.3 to 0.7. In a similar vein, the velocity drops from 19.31 mm s^{-1} to 8.278 mm s^{-1}, or around 11.032 mm s^{-1} at $r = 2$ mm, when viscosity increases from 0.3 to 0.7. At last, as the image illustrates, viscosity increases slightly before velocity first drops quickly and then gradually. As we move toward the center, the velocity gradually increases from zero on the inner wall. A low viscosity causes the velocity to increase more quickly.

Figure 2(D), describes the distribution of velocity for different values of increased viscosity due to the presence of red blood cells. Here $\beta\mathcal{H} = b_2$ takes vlues $(0.5, 1, 1.5, 2)$ and $1 + \beta\mathcal{H} = b_1$ has values $(1.5, 2, 2.5, 3)$. The velocity v at $b_1 = 1.5$ and $b_2 = 0.5$ is 10.57 mm/s. As the b_1 and b_2 increases the velocity decreases and becomes 8.637 mm/s at $b_1 = 2$ and $b_2 = 1$. The velocity at $b_1 = 2.5$ and $b_2 = 1.5$ is 7.863 mm/s for the constant viscosity of plasma 0.5 gram/mm s. The velocity at $b_1 = 3$ and $b_2 = 2$ is (7.186 mm/s for the constant viscosity of plasma (0.5 gram/mm s respectively. It is found that the blood velocity gradually diminishes with increasing increased viscosity due to the presence of red blood cells i.e the flow velocity becomes smaller and smaller as one proceeds away from the center. For equal amount of increases increased viscosity due to the presence of red blood cells of an artery, the velocity in center has maximum and in the inner wall of an artery has minimum.

As we can see from the above figures, effective viscosity has a significant impact on lowering velocity, so include the effective term and increased viscosity due to the presence of red blood cells will yield better results than only considering plasma viscosity.

3.2 Volumetric flow rate in a stenotic artery

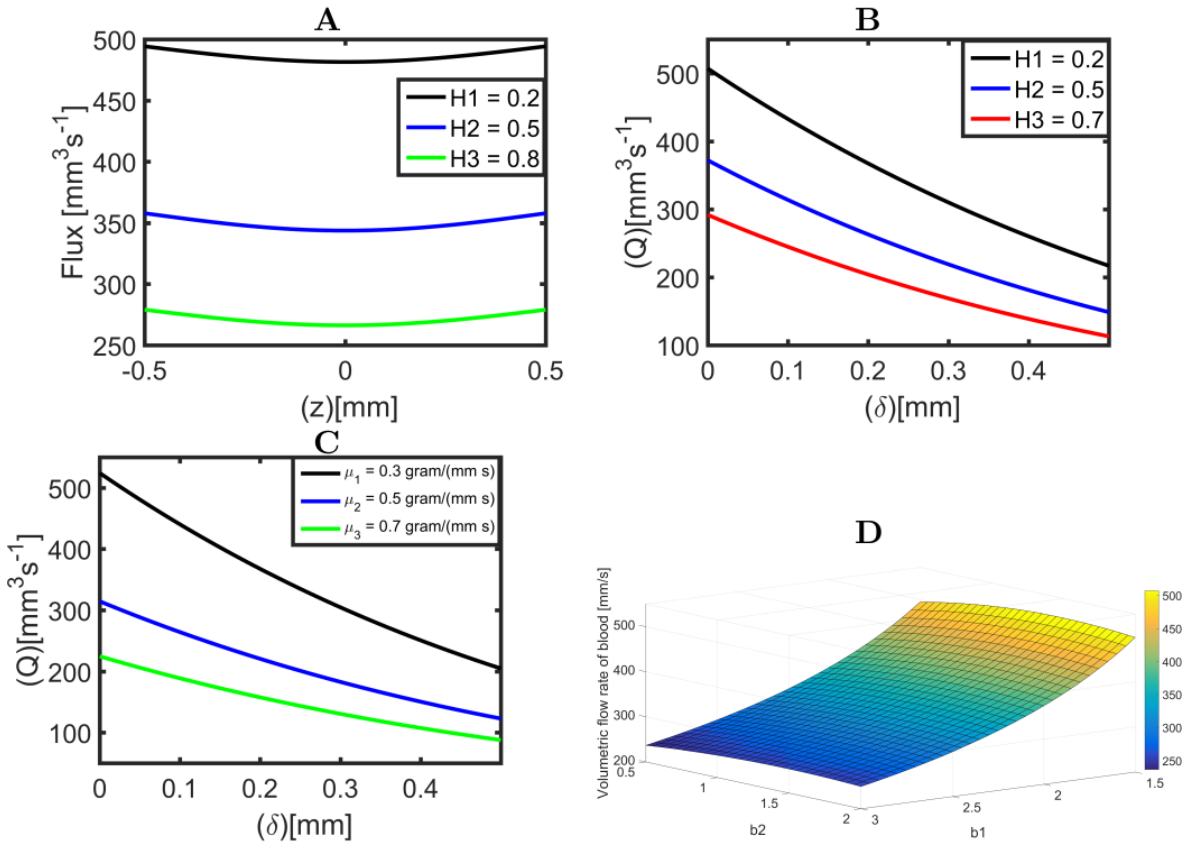

Figure 3: Volumetric flow rate A: at different position of stenosis, B,C: at different height of stenosis, D: increased viscosity due to the presence of red blood cells.

Figure 3(A) explains the volumetric flow rate at various stenosis sites, and several lines are drawn to illustrate the hematocrit values rising. Stenosis positions vary from 0 to 0.5 mm. The volumetric flow rate rises to 494.3 $mm^3\ s^{-1}$ from 481 $mm^3\ s^{-1}$, it is about 13.3 $mm^3\ s^{-1}$ with hematocrit is 0.2, for the position of stenosis from 0 to 0.5. Once more, there is an increase in the volumetric flow rate from 357.8 $mm^3\ s^{-1}$ to 343.7 $mm.^3\ s^{-1}$, the difference is aroud 14.1 $mm^3\ s^{-1}$ at 0.5 for the position of stenosis changes from 0 to 0.5. The volumetric flow rate in the final scenario increases from 266.3 $mm^3\ s^{-1}$ to 279 $mm^3\ s^{-1}$ at 0.7, meaning that the difference in this case is 12.7 $mm^3\ s^{-1}$. We see that there is an inverse relationship between the hematocrit and the volumetric flow rate. Stenosis position and hematocrit together carry a significant danger.

Figure 3(B) is employed to illustrate how, for changing hematocrit, the relationship between volumetric flow rate and height of stenosis varies. Different lines are created for each hematocrit in order to display the influence of hematocrit individually. The highest hematocrit value is 0.7, and the maximum height of stenosis is 0.5 mm. About the time the hematocrit is 0.2 and the stenosis grows from 0 to 0.5 mm, the volumetric flow rate drops from 507 $mm^3\ s^{-1}$ to 216.8 $mm^3\ s^{-1}$. In a similar manner, when the hematocrit value is 0.5, the volumetric flow rate drops from 372 $mm^3\ s^{-1}$ to 148.7 $mm^3\ s^{-1}$. For the hematocrit value of 0.8, the volumetric flow rate drops from 291.8 to 113 $mm^3\ s^{-1}$. While analyzing the variations in the volumetric flow rate decrease, we observe that the variation diminishes as the hematocrit increases. The volumetric flow rate lines are nearly parabolic when the hematocrit values are 0.2, 0.5, and 0.8. This suggests that the stenosis-related change is greatest when hematocrit values are compared. Hematocrit has a greater effect when the stenosis height is less than 0.2 mm. When the stenosis height is greater than 0.4 mm, all of the volumetric flow rate lines fall between 216.8 $mm^3\ s^{-1}$ and 113 $mm^3\ s^{-1}$ for all hematocrit values, indicating a limiting circumstance. This suggests that greater area is required to flow a greater amount, and that in such situation, hematocrit is more effective.

Figure 3(C), explains the relationship, given a range of plasma viscosity values, between volumetric flow rate and thickness of stenosis (δ). To show the impact of varying plasma viscosity, three lines are drawn. In this instance, the constants are hematocrit 0.5, pressure 80 Pa, and radius 3 mm. The volumetric flow rate drops from 524.20 $mm^3\ s^{-1}$ to 204.7$mm^3\ s^{-1}$, when the height of stenosis changes from 0 to 0.5 mm for the viscosity 0.3 gram $mm^{-1}\ s^{-1}$. The volumetric flow rate decreases from 314.5 $mm^3\ s^{-1}$ to 122.8 $mm^3\ s^{-1}$ for the viscosity value of 0.5 gram $mm^{-1}\ s^{-1}$, and from 224.6 $mm^3\ s^{-1}$ to 87.75 $mm^3\ s^{-1}$ approximately for the viscosity value of 0.7 gram $mm^{-1}\ s^{-1}$. In this sense, when viscosity increases, the volumetric flow rate drops. This figure also shows that, when other parameters remain constant and the plasma's viscosity grows uniformly, the volumetric flow rate eventually drops.

Figure 3(D) describes the distribution of volumetric flow rate for increased viscosity due to the presence of red blood cells. Here $b_2 = \beta\mathcal{H}$ and $b_1 = 1 + \beta\mathcal{H}$ takes values $(0.5, 1, 1.5, 2)$ and $(1.5, 2, 2.5, 3)$. The volumetric flow rate at $b_1 = 1.5$ and $b_2 = 0.5$ is 473 mm^3/s. As the increased viscosity due to the presence of red blood cells increases the volumetric flow rate decreases for the constant viscosity and becomes 347.8 $mm^3\ s^{-1}$ at $b_1 = 2$ and $b_2 = 1$. The volumetric flow rate at $b_1 = 2.5$ and $b_2 = 1.5$ is 281.7 mm^3/s for the constant viscosity of plasma 0.5 gram/mm s and becomes 249.3 mm^3/s at $b_1 = 3$ and $b_2 = 2$ for the same viscosity.It is found that the volumetric flow rate gradually diminishes with increasing increased viscosity due to the presence of red blood cells i.e the volumetric flow rate becomes smaller as one proceeds away from the center. For equal amount of increases in increased viscosity due to the presence of red blood cells, the volumetric flow rate at $b_1 = 1.5$, $b_2 = 0.5$ has maximum and at $b_1 = 3$, $b_2 = 2$ has minimum.

3.3 Pressure gradient across the stenosis artery

Figure 4 describes how the ratio of pressure drop to δ varies for varying hematocrit values. Since the gap used to draw these lines is so narrow, the lines appear to be practically linear curves. The pressure drop value ratio is calculated when δ is in the range of 0 and 0.5. The picture illustrates that with a hematocrit of 0.8, the pressure ratio reaches its maximum of approximately 1.323 at $\delta = 0.5$ mm. For the hematocrit value of 0.5, the approximate ratio of pressure drop is 1.296. In the same way, 1.253 for 0.3. When the hematocrit rises within the specified range, the ratio of pressure drop increases steadily. This suggests that as the hematocrit and height of stenosis increase, the ratio of pressure drop increases progressively. The hematocrit measurement may benefit from this knowledge.

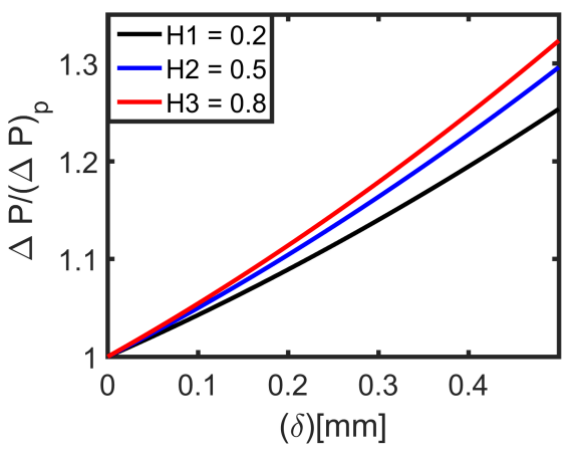

Figure 4: Relation between ratio of Pressure drop for different values of hematocrit with different height of stenosis.

3.4 Shear Stress ratio acroos stenotic artery

Figure 5(A) explains the relationship between the shear stress ratio at various stenosis points, and several curves are produced to illustrate the increasing hematocrit levels. In this case, the stenosis length ranges from -0.5 to 0.5, and its maximal height is found at $z = 0$. Due to the stenosis's symmetric structure, all of the lines symmetrically increase from -0.5 to 0 and decrease after 0. It demonstrates that when stenosis position increases, the ratio of shear stress falls. The ratio of shear stress increases parabolically from the common point to $z = 0$, where it reaches its maximum values 2, 2.096, and 2.144 for the hematocrits of 0.2, 0.5, and 0.8, respectively. When the hematocrit increases shear stress ratio increases gradually. The conclusion from this figure is that the shear stress ratio gets increasingly parabolic and inclines gradually as the hematocrit increases.

Figure 5(B) shows the shear stress ratio at various stenosis heights, with distinct lines being drawn to indicate rising hematocrit values. The highest hematocrit value is 0.8, and the maximum height of stenosis is 0.5 mm. For this reason, every line increases from 0 to 0.5 because the stenosis is thought to have a symmetrical shape. This demonstrates that a uniform rise in the hematocrit also results in a uniform increase in the ratio of shear stress. Shear stress increases and reaches 1.734 at $\delta = 0.5$ mm when the hematocrit is 0.2. At 0.5, the shear stress increases and reaches 1.956 at the maximum height $\delta = 0.5$ mm. At 0.8, the shear stress ratio increases and reaches 2.098, as depicted in the figure. This analysis concludes that as hematocrit increases, the shear stress ratio increases consistently with a uniform quantity. The ratio of shear stress falls as hematocrit decreases, and the curve takes on a parabolic shape at different positions of stenosis. On the other hand, linear curves for various stenosis heights are produced when there is a consistent rise in hematocrit levels along with a uniform increase in the shear stress ratio.

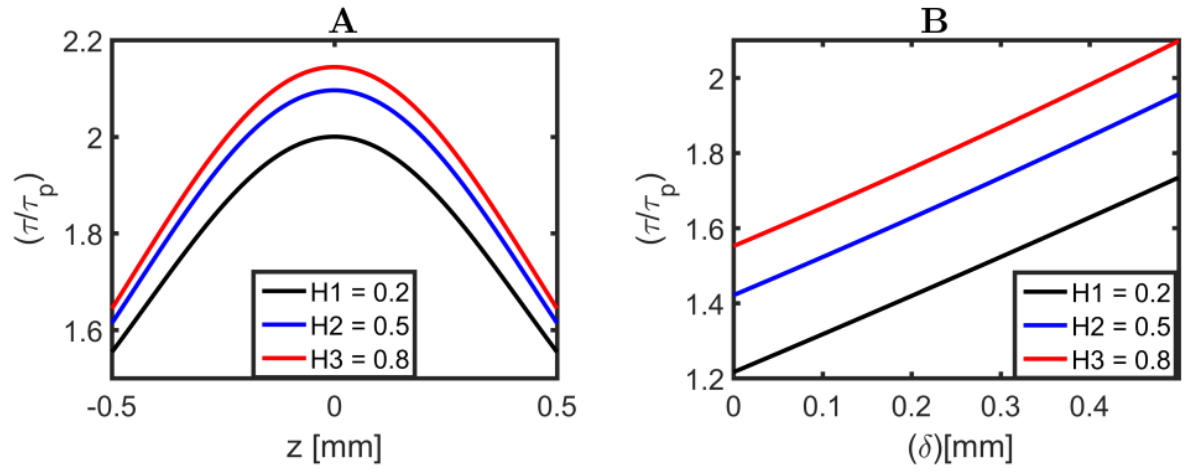

Figure 5: Relation between ratio of the shear stress A: with various position of stenosis for different values of hematocrit, B: at different height of stenosis for different values of viscosity of plasma.

4 Conclusion

Atherosclerotic plaque accumulation and abnormal tissue development lead to stenosis, which restricts blood flow and contributes to cardiovascular diseases like ischemia and stroke. The Einstein coefficient of blood viscosity, which quantifies the resistance to flow in blood vessels, is crucial for understanding hemodynamics and vascular health. Navier-Stokes equations have been applied to ana-

lyze the Einstein viscosity in an axisymmetric direction, calculating model expressions for velocity profile, volumetric flow rate, pressure, pressure drop, and shear stress in an artery. The velocity of blood is more influenced by Einstein's viscosity than plasma viscosity. A significant reduction in volumetric flow rate is observed at the maximum height of stenosis with the uniform increase in hematocrit, indicating a heightened risk of stenosis effects after incorporating effective viscosity. The ratio of pressure drop and shear stress increases linearly with the uniform increase in hematocrit, showing a linear relationship with stenosis height. Blood flow biomechanical modeling holds transformative potential for clinical procedures, surgical outcomes, vascular health understanding, and innovation across bioengineering and medical research, promising enhanced patient outcomes and healthcare advancement.

References

[1] V. A. Nosovitsky, O. J. Ilegbusi, J. Jiang, P. H. Stone, and C. L. Feldman. Effects of curvature and stenosis-like narrowing on wall shear stress in a coronary artery model with phasic flow. *Computers and Biomedical Research*, 30:61–82, 1997.

[2] S. A. Onitilo and M. A. Usman. Effect of multiple stenosis on blood flow in human artery. *Fuw Trends in Science and Technology Journal*, 6(2):643–649, 2021.

[3] C. Pokharel, J. Kafle, and C. R. Bhatta. Analysis of flow characteristics of the blood flow through curved artery with mild stenosis. *Journal of Jilin University (Engineering and Technology Edition)*, 43(3):155–169, 2024.

[4] C. Pokharel, P. N. Gautam, S. T. Tripathee, C. R. Bhatta, and J. Kafle. Analysis of flow parameters in blood flow through mild stenosis. *Nepalese Journal of Zoology*, 6(2):39–44, 2022.

[5] J. N. Pralhad and D. H. Schultz. Modeling of arterial stenosis and its applications to blood diseases. *Mathematical Biosciences*, 190(1):203–220, 2004.

[6] R. Ponalagusamy and R. Machi. A study of a two layered (k.l- newtonian) model of blood flow in an artery with six types of mild stenoses. *Applied Mathematics and Computation*, 367:124767, 2020.

[7] J. H. Forrester and D. F. Young. Flow through a converging-diverging tube and its implications in occlusive vascular disease: a theoretical development. *Journal of Biomechanics*, 3:297–305, 1970.

[8] D. MarDonald. On steady flow through modelled vascular stenosis. *Journal of Biomechanics*, 12:13–20, 1979.

[9] D. F. Young. Effect of a time-dependent stenosis on flow through a tube. *Transactions of the ASME Journal of Engineering for Industry*, 90:248–254, 1968.

[10] S. Chakravarty. Effects of stenosis on the flow-behaviour of blood in an artery. *International Journal of Engineering Science*, 25(8):1003–1016, 1987.

[11] C. Pokharel, P. N. Gautam, C. R. Bhatta, and J. Kafle. Analysis of blood flow through stenosed artery with einstein viscosity. *Journal of Tianjin University Science and Technology*, 57(4):36–52, 2024.

[12] V. P. Srivastava and R. Rastogi. Blood flow through a stenosed catheterized artery: Effects of hematocrit and stenosis shape. *Computers and Mathematics with Applications*, 59(4):1377–1385, 2010.

[13] D. Biswas and U. S. Chakraborty. Impact of hematocrit and slip velocity on pulsatile blood flow in a constricted tapered artery. *International Journal of Engineering Research and Technology*, 3(3):435–449, 2010.

[14] S. A. Onitilo and M. A. Usman. Mathematical analysis of blood flow through a stenosed human artery. *Annals. Computer Science Series*, 16(2):177–185, 2018.

[15] S. A. Onitilo and M. A. Usman. Mathematical modeling of blood flow through a stenosed human carotid artery. *Islamic University Multidisciplinary Journal*, 6(2):178–189, 2019.

[16] A. K. Singh. Effects of shape parameter and length of stenosis on blood flow through improved generalized artery with multiple stenoses. *Advances in Applied Mathematical Biosciences*, 3(1):41–48, 2012.

[17] P. K. Mandal and S. Chakravarty. Numerical study of unsteady flow of non-newtonian fluid through differently shaped arterial stenosis. *International Journal of Computer Mathematics*, 84(7):1059–1077, 2007.

[18] P. R. Chaturani and R. Ponalagusamy. A study of non-newtonian aspects of blood flow through stenosed arteries and its applications in arterial diseases. *Biorheology*, 22:521–531, 1985.

[19] K. Haldar and H. I. Andersson. Two layered model of blood flow through stenosed arteries. *Acta Mechanica*, 117:221–228, 1996.

[20] R. Bali and U. Awasthi. Effects of magnetic field on the resistance to blood flow through stenosed artery. *Applied Mathematics and Computation*, 188:1635–1641, 2007.

[21] J. N. Kapur. *Mathematical models in biology and medicine: Models for blood flows.* Affiliated East-West Press Pvt. Ltd. India, 1985.

[22] M. M. Lih. *Transport phenomenon in medicine and biology*, volume 184. John Wiley and Sons, New York: NY, USA, 1996.